Electromagnetic Transition Rates in ^{58}Ni†

M. C. BERTIN,* N. BENCZER-KOLLER, AND G. G. SEAMAN‡
Rutgers—The State University, New Brunswick, New Jersey 08903
AND
JACK R. MACDONALD
Bell Telephone Laboratories, Murray Hill, New Jersey 07974 and Rutgers—The State University, New Brunswick, New Jersey 08903
(Received 17 February 1969)

Lifetimes of 15 excited states in ^{58}Ni and one in ^{62}Ni have been measured using the Doppler-shift-attenuation method. The levels were excited via inelastic proton scattering at bombarding energies from 7 to 9 MeV. The Doppler shifts of decay γ rays were measured in a 30-cm^3 Ge(Li) detector in coincidence with particles backscattered near 170°. Theoretical estimates of stopping powers were checked experimentally by Doppler-shift-attenuation measurements; excellent agreement was found. The matrix elements extracted from the measured lifetimes are compared with shell-model and vibrational-model predictions. Agreement is, in general, poor. The theoretical analysis indicates that a state-dependent neutron effective charge must be taken into account, and that core excitations play an important role in the determination of transition probabilities.

I. INTRODUCTION

In a simple shell-model description, ^{56}Ni closes the $1f_{7/2}$ shell for both protons and neutrons. Several authors have attempted to explain the structure of the nickel isotopes on the basis of identical nucleon shell-model calculations[1–3] and quasiparticle calculations.[4] In addition, the even nickel isotopes display some of the characteristics of vibrational nuclei: enhanced $E2$ transition rates from the first 2^+ state (2^+_1) to ground, and a triplet of "two-phonon" states of spin and parity 0^+_2, 2^+_2, 4^+_1 at roughly twice the energy of the "one-phonon" state 2^+_1. The vibrational nature of these states has been investigated theoretically by Hsu and French,[5] and Arvieu *et al.*[6] There has been much experimental interest in the even nickel isotopes, and ^{58}Ni in particular has been extensively studied. Spin and parity assignments have been made for most levels in ^{58}Ni below 4.2 MeV[7–12] (see Fig. 1), and the γ-decay modes of the levels of ^{58}Ni have been established.[7–10]

Electromagnetic transition probabilities provide a stringent test of the nuclear models used to describe the nickel isotopes, as they are especially sensitive to small admixtures of configurations in the wave functions. These transition matrix elements are more meaningfully compared with theoretical predictions than, for example, matrix elements obtained from inelastic α-particle scattering, which are dependent on assumptions made about the nuclear-reaction mechanisms.

The lifetimes of the first excited states of the even-even nickel isotopes range from 8×10^{-13} to 2×10^{-12} sec.[13,14] These transitions are enhanced over the Weisskopf single-particle estimates by, roughly, a factor of 10. If the transitions from members of the "two-phonon" triplet to the first excited state are enhanced by a factor of 20, then the lifetimes of these states will lie between 10^{-13} and 10^{-11} sec. In addition, shell-model single-particle estimates of the lifetimes of these and many other states range from 10^{-14} to 10^{-11} sec. In this region of nuclear lifetimes, the Doppler-shift-attenuation method (DSA) is applicable. The lifetimes of 15 states in ^{58}Ni were so measured, and a lower limit was set for one other state. A preliminary report on part of this work has already been published.[15] The lifetime of the 2^+_2 state of ^{62}Ni was measured, and a lower limit was set on the lifetime of the 2^+_2 state of ^{60}Ni. Matrix elements were extracted from the combined lifetime and decay-scheme data. The energies of γ rays produced in the ^{58}Ni(p, $p'\gamma$) reaction were measured with a Ge(Li) detector, and the ^{58}Ni level energies were precisely determined.

II. DOPPLER-SHIFT-ATTENUATION METHOD

A. Description of Method

The DSA method compares the lifetime of a moving nucleus with the slowing-down time of the nucleus in

† Work supported in part by the National Science Foundation.
* Present address: Department of Physics, Stanford University, Palo Alto, Calif.
‡ Present address: Department of Physics, Kansas State University, Manhattan, Kan.
[1] S. Cohen, R. D. Lawson, M. H. MacFarlane, S. Pandya, and M. Soga, Phys. Rev. **160**, 903 (1967).
[2] N. Auerbach, Phys. Rev. **163**, 1203 (1967).
[3] Y. K. Gambhir and Ram Raj, Phys. Rev. **161**, 1125 (1967).
[4] Ram Raj, Y. K. Gambhir, and M. K. Pal, Phys. Rev. **163**, 1004 (1967).
[5] L. S. Hsu and J. B. French, Phys. Letters **19**, 135 (1965).
[6] R. Arvieu, E. Salusti, and M. Veneroni, Phys. Letters **8**, 334 (1964); R. Arvieu and E. Salusti, Nucl. Phys. **66**, 305 (1965).
[7] D. F. H. Start, M. A. Grace, J. R. MacDonald, and R. Anderson (private communication).
[8] D. M. Van Patter, R. N. Horoshko, and P. F. Hinrichsen (private communication); Bull. Am. Phys. Soc. **12**, 1034 (1967); D. M. Van Patter, H. L. Scott, and R. N. Horoshko, *ibid.* **13**, 724 (1968).
[9] R. N. Horoshko, P. F. Hinrichsen, L. W. Swenson, and D. M. Van Patter, Nucl. Phys. **A104**, 113 (1967).
[10] P. F. Hinrichsen, G. T. Wood, and S. M. Shafroth, Nucl. Phys. **81**, 449 (1966).
[11] L. W. Swenson and R. K. Mohindra, Phys. Rev. **150**, 877 (1966).
[12] O. N. Jarvis, B. G. Harvey, D. L. Hendrie, and J. Mahoney, Nucl. Phys. **A102**, 625 (1967).
[13] P. H. Stelson and F. K. McGowan, Nucl. Phys. **32**, 652 (1962).
[14] D. S. Andreyev, N. P. Grinberg, K. I. Erokhina, and I. K. Lemberg, Nucl. Phys. **19**, 400 (1960).
[15] M. C. Bertin, N. Benczer-Koller, G. G. Seaman, and J. R. MacDonald, Phys. Letters **26B**, 623 (1968).

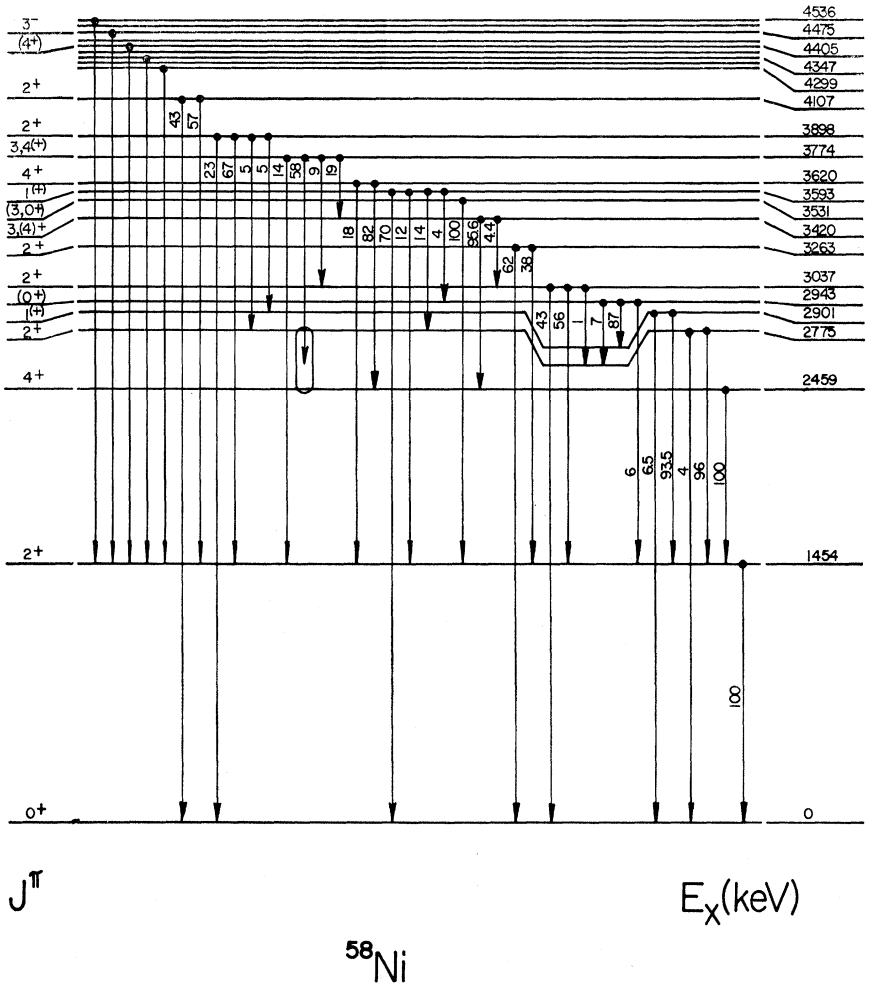

FIG. 1. ^{58}Ni level scheme and electromagnetic decay modes. The decay shown for the 4.107-MeV level is that of Ref. 8. Other decay modes are averages of data from Refs. 7–10.

the matter through which it is moving. If the lifetime is long compared to the slowing-down time, most of the excited nuclei decay at rest. If the lifetime is very short compared to the slowing-down time, the nuclei decay in flight before slowing down. In the former case, there is little change in γ-ray energy due to the Doppler effect, while in the latter case one observes the maximum Doppler shift. For an intermediate case the observed energy shift is a function of the lifetime, and in this region the DSA method is most useful. The slowing-down times of nuclei in solids depend on the ion-stopping medium combination, and the initial energy of the ion. Typically, however, these times are on the order of 5×10^{-13} sec, and one can measure lifetimes an order of magnitude longer or shorter than this. The many variations and the details of the method have been discussed by other authors.[16–19]

In the present experiments, the centroid-shift variant of the DSA method was applied. γ-ray spectra were observed at two γ-detector angles in coincidence with protons,[19] α particles, or ^{16}O ions inelastically backscattered from the level studied. A schematic of the experimental arrangement is shown in Fig. 2. From the centroid shift of the γ-ray lines, the attenuation factor $F(\tau)$ was determined. $F(\tau)$ is the ratio of the observed shift to the maximum possible shift and is defined below for v_i much smaller than c:

$$F(\tau)=\frac{\Delta E}{E_{\gamma 0}\langle v_i/c\rangle(\cos\theta_1-\cos\theta_2)}. \qquad (2.1)$$

Here $E_{\gamma 0}$ is the unshifted γ-ray energy, ΔE is the centroid shift, $\langle v_i\rangle$ is the initial recoil velocity of the nucleus averaged over finite target thickness and detector solid angle, θ_1 and θ_2 are the angles between the recoil direction and the direction of γ-ray emission, and τ is the mean life of the state under study. In the present coincidence experiments, both the magnitude and direction of v_i were precisely defined.

To extract lifetime information from the measured attenuation factor, one must be able to calculate the dependence of $F(\tau)$ on the lifetime τ. The average

[16] S. Devons, G. Manning, and D. ST. P. Bunbury, Proc. Roy. Soc. (London) **A68**, 18 (1954).
[17] A. E. Litherland, M. J. L. Yates, B. M. Hinds, and D. Eccleshall, Nucl. Phys. **44**, 220 (1963).
[18] E. K. Warburton, J. W. Olness, and A. R. Poletti, Phys. Rev. **160**, 938 (1967).
[19] J. R. MacDonald, D. F. H. Start, R. Anderson, A. G. Robertson, and M. A. Grace, Nucl. Phys. **A113**, 6 (1968).

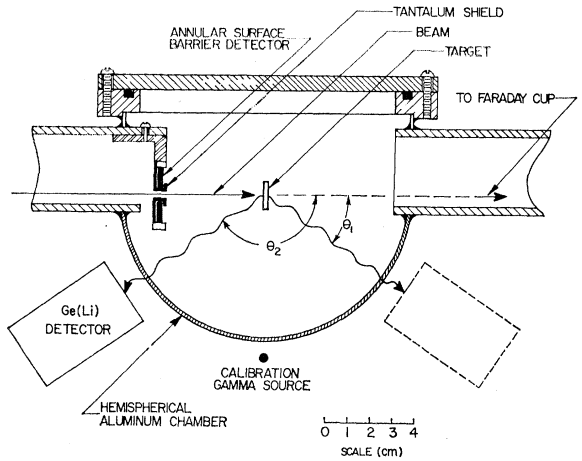

FIG. 2. Schematic of the experimental arrangement.

energy (peak centroid energy) of γ rays emitted from an ensemble of nuclei decaying exponentially as a function of time after excitation is

$$\bar{E}_\gamma = E_{\gamma 0}[1+(v_i/c)F(\tau)\cos\theta], \qquad (2.2)$$

where

$$F(\tau) = \frac{1}{v_i\tau}\int_0^\infty v(t)\cos\phi_b(t)\, e^{-t/\tau}dt. \qquad (2.3)$$

The $\cos\phi_b$ term accounts for deflections from the initial recoil direction. The attenuation factor Eq. (2.3) can be rewritten as an energy integral:

$$F(\tau) = \frac{1}{v_i\tau}\int_{E_i}^0 \frac{\cos\phi_b(E)\, e^{-t(E)/\tau}dE}{dE/dx}. \qquad (2.3')$$

The $F(\tau)$ calculated from Eq. (2.3′) must be averaged to include the effects of target thickness and particle-detector solid angle on the initial ion-recoil energy E_i and velocity v_i. To evaluate expression (2.3′), the stopping power theory due to Lindhard, Scharff, and Schiøtt[20] (hereafter referred to as LSS) was applied. Large-angle scattering was treated according to a method outlined by Blaugrund.[21]

B. Stopping Cross Sections

A heavy ion (A_1, Z_1) slowing down in matter (A_2, Z_2) loses energy in collisions with electrons of the stopping material and with atoms as a whole (nuclear collisions). At velocities much greater than $v_0 = c/137$ (the velocity of an electron in the first Bohr orbit of hydrogen) the electronic energy-loss mechanism is dominant, and the collisions involve small energy transfer and negligible scattering. At ion velocities below v_0 a large fraction of the ion's energy is lost in nuclear collisions. These "hard" collisions may involve large energy losses and large-angle scattering. The electronic stopping cross section has been assumed to be directly proportional to the ion's velocity as predicted by LSS. The proportionality constant was determined by interpolation between existing energy loss data for heavy ions in nickel.[21–24] The constant used was 1.04 times the value predicted by LSS. The nuclear-stopping cross section used was that calculated by LSS from a Thomas-Fermi ion-atom potential. The nuclear specific energy-loss function is published in graph form, Fig. 2 of LSS, and is tabulated by Schiøtt.[25] This function can be approximated by the expression

$$d\epsilon/d\rho_n = \epsilon^{1/2}/(0.67+2.07\epsilon+0.03\epsilon^2), \qquad (2.4)$$

where ϵ and ρ are the dimensionless energy and length parameters defined by LSS. Lieb *et al.*[26] suggested a similar expression without a quadratic term in the denominator; expression (2.4) gives a better fit to $d\epsilon/d\rho_n$ over a wider range of ϵ. The functional form of Eq. (2.4) is particularly useful, because it simplifies many of the expressions appearing in the calculation of the attenuation factor (2.3′). The scattering terms, $\cos\phi_b(E)$ and $\exp[-t(E)/\tau]$ can be evaluated analytically, and while $F(\tau)$ itself cannot be obtained analytically, the numerical integration is greatly simplified. Recoil-ion ranges and the fraction of energy lost by the primary ion in electronic collisions can also be calculated with this expression. Figure 3 shows the electronic and nuclear energy-loss functions for ^{58}Ni ions recoiling in a ^{58}Ni stopping medium.

C. Experimental Check of Theoretical Stopping Cross-Section Predictions

To check the validity of the LSS predictions for electronic and nuclear stopping, a lifetime which had

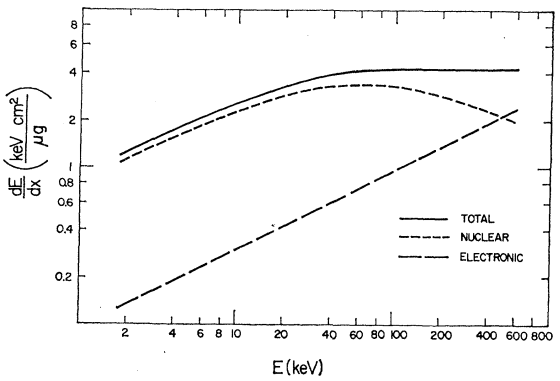

FIG. 3. Electronic and nuclear stopping powers for ^{58}Ni ions recoiling in a ^{58}Ni stopping medium.

[20] J. Lindhard, M. Scharff, and H. E. Schiøtt, Kgl. Danske Videnskab. Selskab, Mat.-Fys. Medd. **33**, No. 14 (1963).
[21] A. E. Blaugrund, Nucl. Phys. **88**, 501 (1966).
[22] C. D. Moak and M. D. Brown, Phys. Rev. Letters **11**, 284 (1963); Phys. Rev. **149**, 724 (1966); L. B. Bridwell, L. C. Northcliffe, S. Datz, C. D. Moak, and H. O. Lutz, *ibid.* **159**, 276 (1967).
[23] W. Booth and I. S. Grant, Nucl. Phys. **63**, 481 (1965).
[24] D. I. Porat and K. Ramayataran, Proc. Phys. Soc. (London) **77**, 97 (1961); **78**, 1135 (1961).
[25] H. G. Schiøtt, Kgl. Danske Videnskab. Selskab, Mat.-Fys. Medd. **35**, No. 9 (1966).
[26] K. P. Lieb, H. Grawe, and H. Ropke, Nucl. Phys. **A98**, 145 (1967).

already been determined by other methods was measured. The first excited state of ^{58}Ni, a 2^+ state at 1.454 MeV was chosen for this purpose. Its reduced transition probability $B(E2: 0^+_1 \rightarrow 2^+_1)$ has been measured by Coulomb excitation with α particles.[13] The value of this $B(E2)$ is $(730\pm80)\ e^2\ \mathrm{fm}^4$ corresponding to a mean life of $(8.6\pm0.9)\times10^{-13}$ sec, well within the range of the Doppler-shift method. The aim of the experiment was to vary the relative amounts of electronic and nuclear energy loss suffered by the ^{58}Ni recoil ion and compare the lifetimes measured under these different experimental conditions. As the initial recoil energy E_i of the ^{58}Ni ion increases, the fraction of the energy loss which is nuclear, E_n/E_i, decreases. To achieve the necessary recoil velocities, the state was excited by inelastic scattering of protons, α particles, and ^{16}O ions. The recoil ions were stopped in the target itself. The experiments were coincidence measurements and are described in Sec. III.

The lifetime was determined from the $F(\tau)$ curves shown in Fig. 4. The effect of decreasing initial recoil energy E_i is clearly displayed on a semilog plot. The curve almost translates toward decreasing τ with decreasing E_i. Table I shows the projectile, bombarding energy, initial recoil energy, fractional nuclear energy loss, and lifetime measured. The errors shown include statistical uncertainty, as well as uncertainties in beam energy and detector position. Even though E_n/E_i varied by more than a factor of 10, these measurements agreed with each other, and with the Coulomb excitation measurement of the lifetime. Therefore, it was felt that the LSS-Blaugrund method was valid for analyzing the DSA data. A change in the stopping cross sections of $\pm15\%$ would have yielded lifetimes inconsistent with the Coulomb excitation result. A $\pm15\%$ error was assumed for the dE/dx expressions, and the contribution to the total error from this source was determined as described in Sec. III C.

III. MEASUREMENT OF DOPPLER SHIFTS

A. Experimental Arrangement

Protons, α particles, and ^{16}O ions accelerated in the Rutgers-Bell Model FN Tandem were used to excite

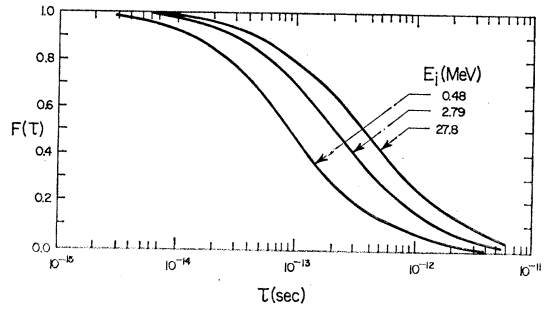

FIG. 4. $F(\tau)$ curves corresponding to ^{58}Ni ions recoiling with various initial energies after bombardment with protons, α particles, or oxygen ions.

TABLE I. Comparison of the lifetime of the 1.454-MeV (2^+) state of ^{58}Ni obtained from Doppler-shift-attenuation measurements with different recoil velocities. The assigned errors are purely statistical.

Reaction	Bombarding energy (MeV)	Initial recoil energy (MeV)	Nuclear energy loss: Total energy loss	τ_m(fsec)
(p, p')	8.08	0.48	0.67	890_{-130}^{+210}
(α, α')	12.16	2.79	0.34	870_{-130}^{+200}
$(^{16}O, ^{16}O')$	42.0	27.8	0.06	1020_{-130}^{+220}
Weighted average				920_{-75}^{+120}
Coulomb excitation[a]				862 ± 90

[a] Reference 13.

the states under study. The γ rays were detected in an Ortec 30-cm^3 cylindrical Ge(Li) detector in coincidence with particles backscattered into an annular surface-barrier Si detector, subtending an average angle $\langle\theta\rangle=170°$ with respect to the beam. A schematic of the apparatus is shown in Fig. 2. The targets used were 99% enriched foils of ^{58,60,62}Ni prepared by electroplating onto a copper backing. The copper backings were then etched away, leaving a self-supporting nickel foil. The targets used for the lifetime measurements were typically between 2 and 4 mg/cm^2 thick. For the ^{16}O measurement of the lifetime of the first excited state of ^{58}Ni, a 7.5-mg/cm^2 target was employed.

A fast-slow coincidence circuit with a time-to-amplitude converter (TAC) was used. A block diagram of the electronic circuits is shown in Fig. 5. Timing resolution in the TAC spectrum was about 9 nsec full width at half-maximum (FWHM) for a γ-ray energy window of 1.2–4.2 MeV. The precision servopulser of the Bell Laboratories 4096-channel analog-to-digital converter (ADC)[27] was used to gain-stabilize the electronics, and the data were stored in an SDS 910 on-line computer system via a multichannel analyzer program. A spectrum of random coincidences between a variable frequency pulser and the γ-ray counter was stored in one portion of the analyzer. Appropriately chosen radioactive sources were located near the detector, and the positions of the source calibration lines in the random coincidence spectrum were used to make unambiguous corrections for any gain shifts or zero drifts. These shifts were usually negligible and in the worst case, less than 1.0 keV. Figure 6 shows pulser-γ coincidence spectra which include the 1.274-MeV γ ray from a ^{22}Na source. These spectra, which were accumulated during a 16-h measurement of the lifetime of the 1.454-MeV level of ^{58}Ni, show an energy resolution of less than 6 keV and a gain shift of 0.1 keV. This

[27] E. A. Gere and G. L. Miller, IEEE Trans. Nucl. Sci. **NS-13**, 508 (1966).

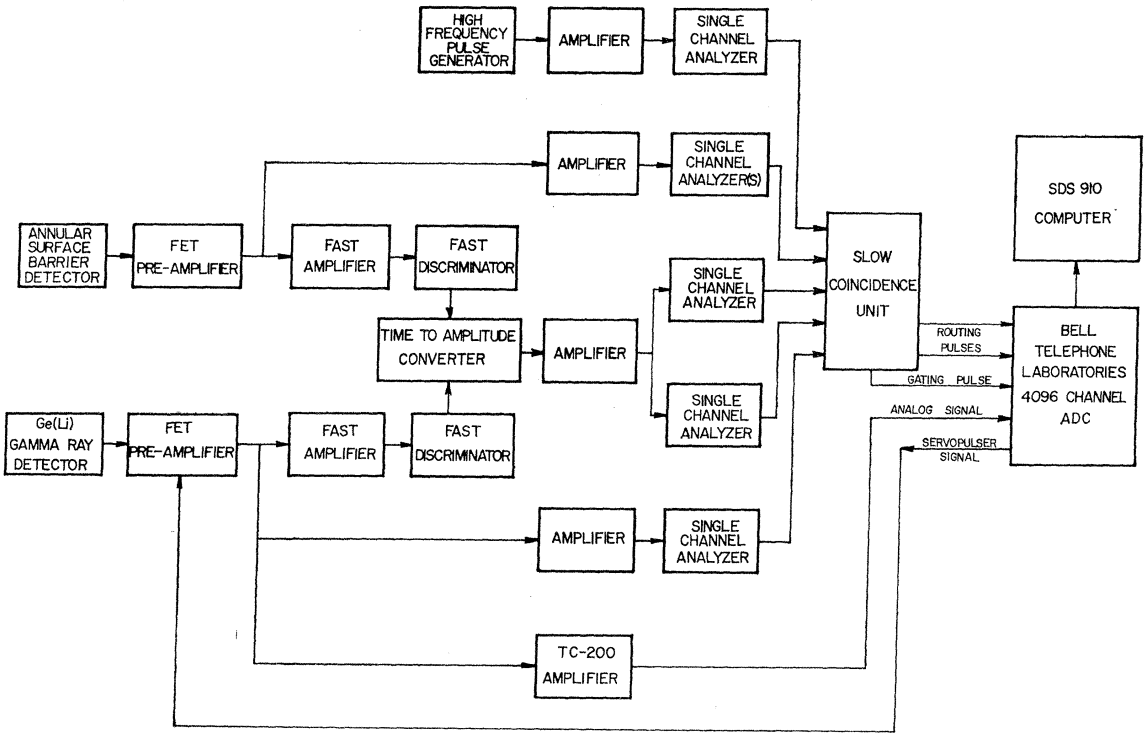

FIG. 5. Block diagram of the electronic circuits.

method of storing a "singles" spectrum avoids the dead-time losses associated with the true singles rate, which in the above case was 12 000 counts/sec. Figure 7 shows the coincidence spectra of the 1.454-MeV γ ray of ^{58}Ni; the observed centroid shift is (0.79±0.13) keV.

The 4096-channel analyzer program was used in a 2×2048 mode to study γ rays from one level (one-particle–γ coincidence spectrum and the pulser-γ coincidence spectrum), or a 4×1024 mode to study γ rays from three separate levels simultaneously. "Random" spectra were not recorded in the analyzer, but were simulated by normalizing the " singles" spectrum to the total number of random events as recorded on a scaler. The total spectrum true-to-random ratio was typically 15 to 1. However, near peaks of interest random counts were usually negligible.

B. Excitation Functions

In order to determine the beam energies at which to perform the lifetime experiments, excitation functions were measured for ^{58,60,62}Ni in the proton energy range 7–9 MeV, for ^{58}Ni in the α-particle energy range 10–16 MeV, and the ^{16}O ion energy range 24–42 MeV. Self-supporting nickel foils of typical thickness 200 μg/cm^2 were used for these measurements. The Ni(p, p') cross sections for scattering to 170° were found to vary by as much as an order of magnitude over energy ranges of a few keV. Using the excitation-function data, it was possible to choose bombarding energies at which the yields from the levels under study were maximized.

The large initial recoil velocities resulting from inelastic oxygen ion scattering makes ^{16}O a very desirable projectile to use for DSA measurements. The inelastic and elastic scattering cross sections of ^{16}O ions from ^{58}Ni were studied between 24 and 42 MeV, and a preliminary report of these data has been presented.[28] Below 32 MeV the energy dependence of the ^{58}Ni(^{16}O, ^{16}O$'\gamma$) cross section for scattering from the 1.45-MeV (2^+_1) state of ^{58}Ni is that predicted by Coulomb excitation theory. The cross section for inelastic scattering to 170° was too small to make particle-γ coincidence measurements with a Ge(Li) detector feasible. Above 32 MeV, the inelastic scattering cross section lies below the theoretical prediction. It reaches a minimum near 36 MeV, then rises sharply to a maximum at 42 MeV. Similar behavior has been noted in the cross sections for scattering from the first three excited states of ^{63}Cu, and for two states in ^{117}Sn.[29] This effect is, at present, unexplained. At 42 MeV, the cross section for inelastic ^{16}O ion scattering from the 2^+_1 state of ^{58}Ni was greater than 1 mb/sr, and was large enough to permit the lifetime measurement to be performed. It should also be noted that higher states in ^{58}Ni were not excited.

[28] G. G. Seaman, M. C. Bertin, and N. Benczer-Koller, Bull. Am. Phys. Soc. **12**, 491 (1967).

[29] M. C. Bertin, Ph.D. thesis, Rutgers–The State University, 1968 (unpublished).

C. Data Acquisition and Analysis

The nickel recoil ions produced by inelastic proton scattering had an average initial energy of 450 keV. The range of these nuclei in the nickel stopping medium is on the order of 100 μg/cm^2. In order to evaluate the attenuation factor, Eq. (2.3), the velocity of the recoil ions must be known as a function of time. If these ions are stopped in the target, the LSS stopping cross sections can be used in Eq. (2.3′) to calculate $F(\tau)$. If, on the other hand, the recoil ions escape from the target into vacuum, the γ rays emitted from these nuclei will have a larger Doppler shift, and the results of the measurement will yield a lifetime shorter than the actual lifetime. A stringent energy window on the backscattered proton groups insured that all the coincidence γ rays came from nuclei excited near the front of the target. Figure 8 shows spectra of protons backscattered from 0.2- and 3.6-mg/cm^2 ^{58}Ni targets at a proton bombarding energy of 8.908 MeV. The thin target was used to set an energy window on protons scattered from a given level. The 3.90-MeV level is illustrated in the figure.

The centroid analysis of the γ-ray spectra was performed with the aid of the light pen facility of the Rutgers SDS 925 computer. In cases where both full-energy and double-escape peaks were present in the spectrum, or where a state decayed in more than one way, several independent measurements of the attenuation factor were obtained. For example, spectra of Doppler-shifted γ rays from the decay of the 3.90-MeV level of ^{58}Ni are shown in Fig. 9. This state decays strongly to both the ground and first excited states, allowing four separate determinations of $F(\tau)$.

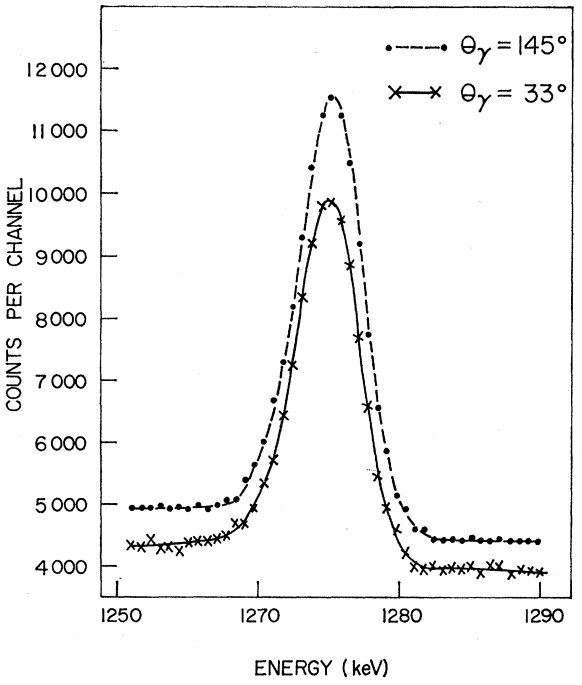

FIG. 6. Pulser-γ coincidence spectrum showing the 1.274-MeV calibration line from a ^{22}Na source.

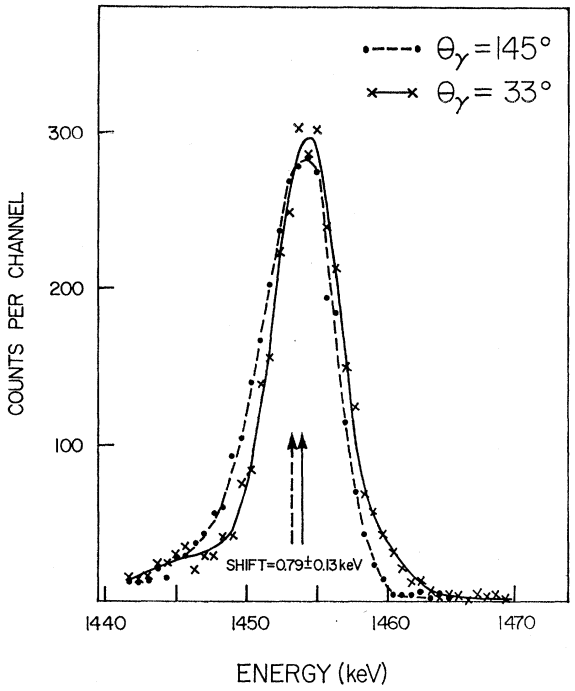

FIG. 7. Doppler-shifted spectra of the 1.454-MeV γ-ray peak observed at 33° and 145° in coincidence with backscattered protons.

Two types of errors contribute to the lifetime obtained from a DSA measurement. The first of these is simply the error in the measured $F(\tau)$, Eq. (2.1), which arises primarily from the statistical uncertainty in the determination of the centroid shift ΔE. Uncertainties in the initial recoil velocity $\langle v_i \rangle$ and detector angles make small contributions to this error. The second type of error is associated with uncertainties in the stopping cross sections used to evaluate the "theoretical" attenuation factor, Eq. (2.3′). The treatment of this problem is discussed in the Appendix. The errors in τ due to uncertainties in the measured $F(\tau)$ and those due to uncertainties in the calculation of the $F(\tau)$ curve were added in quadrature to obtain the total error in τ. In cases where a lifetime was measured more than once, the individual measurements were weighted inversely as the square of their absolute error, and this weighted average was adopted as the final value.

IV. RESULTS

A. Lifetimes and γ-Ray Energies

The energies of γ rays emitted in the ^{58}Ni(p, $p'\gamma$) reaction were determined in a "singles" experiment using a 4096 multichannel analyzer program to cover the energy range 0.8–4.2 MeV. The Ge(Li) detector

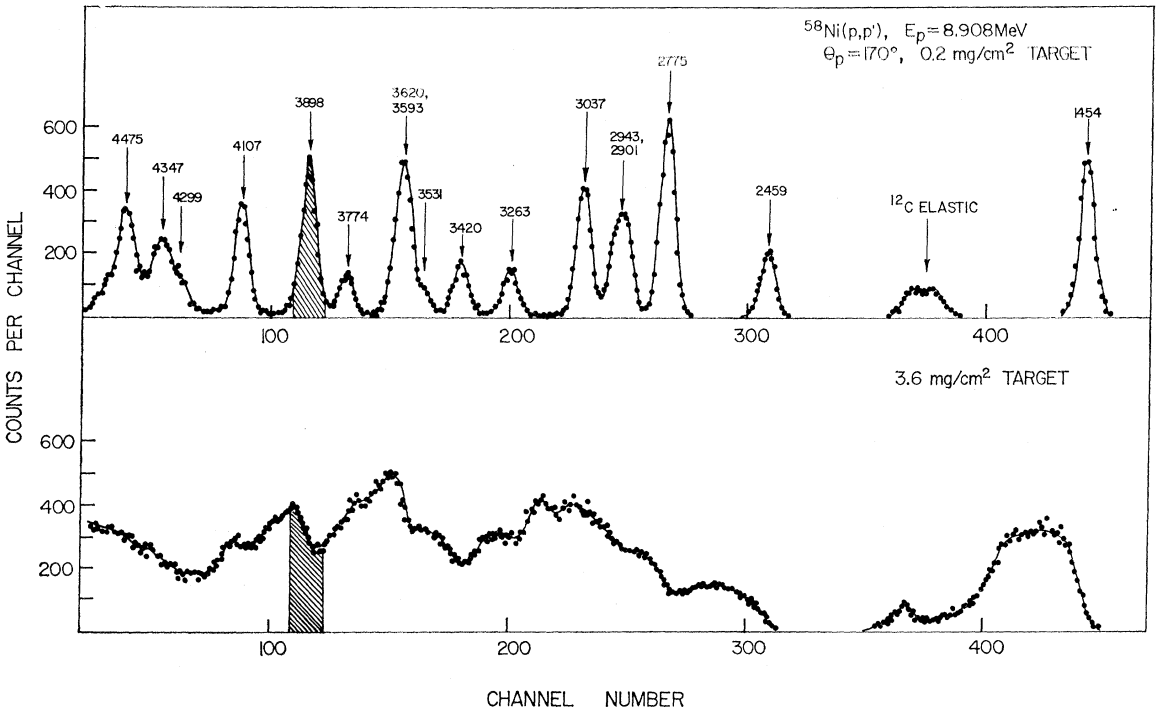

FIG. 8. Spectra of protons backscattered from ^{58}Ni targets 0.2 and 3.6 mg/cm^2 thick at E_p=8.908 MeV. The shaded area indicates a typical energy window.

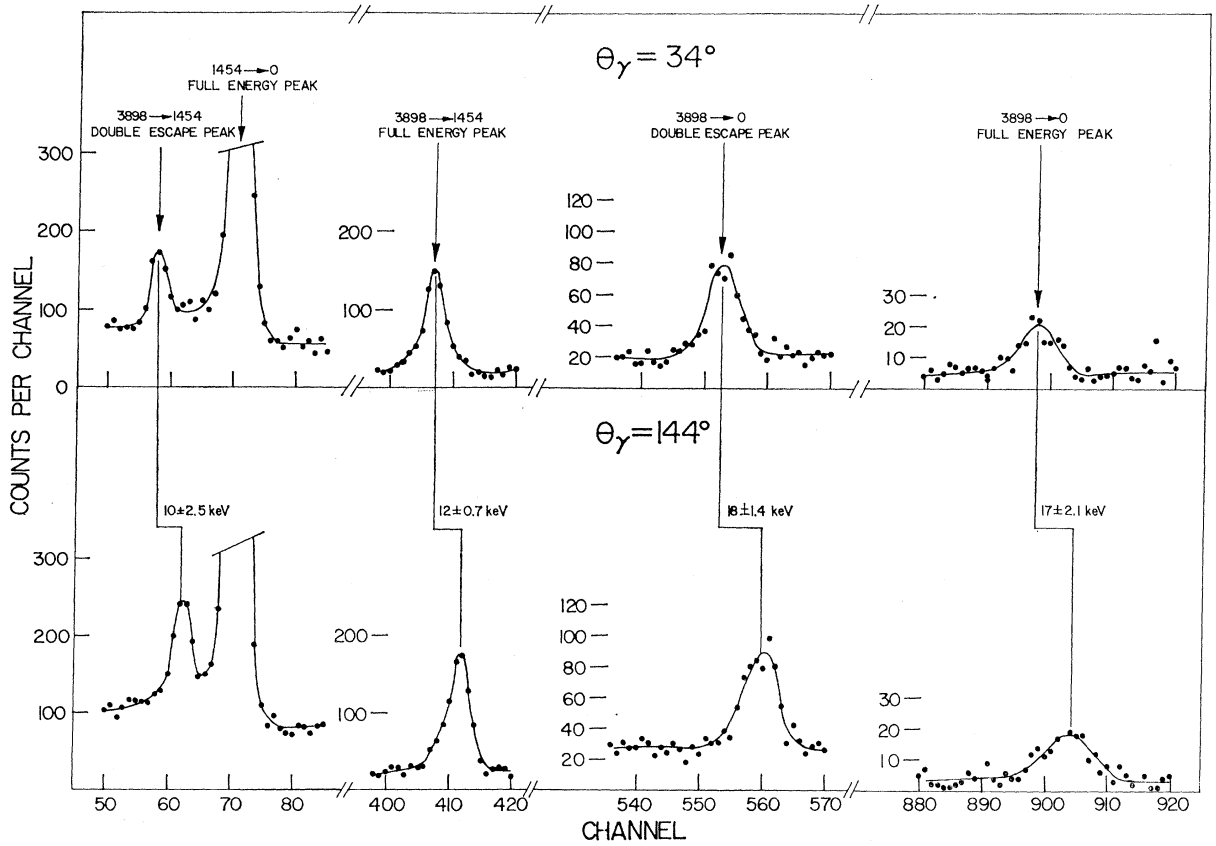

FIG. 9. Doppler-shifted full-energy and double-escape peaks from the cascade and cross over decay of the 3.898-MeV state.

TABLE II. Summary of the level energies (the error in the last figure is in parentheses), proton bombarding energies, measured attenuation factors $F(\tau)$, and lifetimes τ for states in ^{58}Ni, ^{60}Ni, and ^{62}Ni.

Nucleus	Level	Energy (keV)	Proton bombarding energy (MeV)	Measured $F(\tau)$	τ_m (fsec)
^{58}N	1	1454.1(4)	8.08	0.080±0.013	920_{-100}^{+140} [a]
	2	2459.2(6)	8.19	<0.05	>1400
	3	2774.7(6)	8.35	0.12±0.05	550_{-130}^{+180}
	4	2901.1(6)			90±35 [b]
	5	2942.6(9)			(2.8±0.1)×10^6 [b]
	6	3037.2(6)	8.98	0.63±0.05	57_{-7}^{+8}
			8.35	0.62±0.03	
	7	3263.1(5)	8.35	0.73±0.02	36±5
			8.78	0.73±0.03	
	8	3420.3(8)	8.19	0.16±0.07	380_{-140}^{+320}
			8.78	0.20±0.06	
	9	3531.0(9)	8.78	0.22±0.04	280±80
	10	3593.3(9)	8.78	0.66±0.04	48_{-11}^{+13}
	11	3619.7(9)	8.78	0.34±0.11	160_{-70}^{+120}
	12	3773.8(14)			400_{-100}^{+2000}
	13	3897.7(5)	8.91	0.74±0.03	33±4
			8.93	0.76±0.02	
	14	4106.8(6)	8.93	0.47±0.02	94±14
	15	4299.3(42)	8.78	0.74±0.19	34_{-26}^{+31}
	17	4346.6(15)	8.78	0.79±0.20	24_{-18}^{+22}
	19	4404.8(13)	8.78	0.58±0.09	62_{-20}^{+24}
	21	4475.3(8)	8.78	0.78±0.07	27±11
	23	4536.1(8)	8.78	0.67±0.07	45±15
^{60}Ni	2	2160(3)	6.94	<0.04	>2000
^{62}Ni	3	2300(3)	7.87	0.066±0.016	1100_{-270}^{+410}

[a] Weighted average of the three measurements performed with p, α, and ^{16}O ions.
[b] Reference 32.

was placed at 90° to the beam direction so that the γ-ray lines would not be Doppler shifted. Radioactive sources of ^{88}Y (0.89801 and 1.83608 MeV),[30] ^{22}Na (1.27452 MeV),[30] and RaTh (2.61447 MeV)[31] placed near the detector during the run provided calibration lines in the spectrum. A quadratic least-squares fit of peak channel versus energy was used to determine the energies between 0.8 and 3.2 MeV, which included either the full-energy or double-escape peaks of all γ rays observed.

γ rays from two transitions, 2.901→1.454 MeV and 3.773→2.459 MeV, appear in the singles spectrum as small tails on other larger peaks. The final energy determinations for these γ rays were made from coincidence spectra accumulated during the lifetime measurements. The energies of γ rays from states at 4.299, 4.346, and 4.404 MeV were also obtained from coincidence measurements.

The level energies, proton bombarding energies, measured attenuation factors $F(\tau)$, and lifetimes τ are summarized in Table II. The level energies were deduced from the γ-ray energies using the known decay scheme.[7–10] Agreement with level energy measurements made by inelastic proton scattering[32] and other Ge(Li) detector γ-ray studies[33,8] is good. The

[30] W. W. Black and R. L. Heath, Nucl. Phys. **A90**, 650 (1967).
[31] G. Murray, R. L. Graham, and J. S. Geiger, Nucl. Phys. **63**, 353 (1965).
[32] R. G. Tee and A. Aspinall, Nucl. Phys. **A98**, 417 (1967); E. R. Cosman, C. H. Paris, A. Sperduto, and H. A. Enge, Phys. Rev. **142**, 673 (1966).
[33] D. F. H. Start, R. Anderson, A. G. Robertson, and M. A. Grace (private communication).

TABLE III. Summary of the decay properties of states in ^{58}Ni and of the second 2^+ levels in ^{60}Ni and ^{62}Ni.

Level	J^π	Level energy (keV)	Decay mode % decay	To level	Multipole mixing ratio	σL	$\lvert M\rvert^2$ [Weisskopf units (W.u.)]	$B(E2)$ (e^2 fm^4)
1	2^+	1454	100	0		$E2$	10.0±1.3	136±18
2	4^+	2459	100	1	0.0±0.1	$E2$	<41	<560
3	2^+	2775	4±1	0		$E2$	$(2.7\pm1.0)\times10^{-2}$	0.36±0.14
			96±1	1	1.12±0.2	$E2$	14.5±5.0	200±70
						$M1$	$(1.1\pm0.4)\times10^{-2}$	
4[a]	1^+	2901	6.5±1	0		$M1$	$(9.4_{-3}^{+6})\times10^{-4}$	
			93.5±1	1		if $M1$	$0.11_{-0.03}^{+0.07}$	
5[a]	0^+	2943	6±2	1		$E2$	$(1.8\pm0.6)\times10^{-4}$	$(2.4\pm0.8)\times10^{-3}$
			7±1	3		$E2$	11.1±1.6	150±22
			87±2	4		$M1$	0.13±0.005	
6	2^+	3037	43±4	0		$E2$	1.7±0.3	24±4
			56±3	1	−0.18±0.06	$E2$	1.9±1.3	26±18
						$M1$	$(7.5\pm1.0)\times10^{-2}$	
			1.0±0.2	3		$(M1)$	0.31±0.08	
7	2^+	3263	63±2	0		$E2$	2.8±0.5	38±6
			37±2	1	−0.67±0.25	$E2$	10±5	140±70
						$M1$	$(3.8\pm1.1)\times10^{-2}$	
			≤0.2	3		$(M1)$	$\leq2\times10^{-2}$	
			≤0.2	4		$(M1)$	$\leq4\times10^{-2}$	
8	$3(4)^+$	3420	95.6±1	2	0.0±0.1	$M1$	$(9.5)\times10^{-2}$	
			≤1.1	3		$(M1)$	$\leq5\times10^{-3}$	
			4.4±1	6		(M1)	$(6\pm4)\times10^{-2}$	
9	(0^+)	3531	100	1		$(E2)$	$5.5_{-1.2}^{+2.2}$	75_{-16}^{+30}
10	1^+	3593	70±3	0		$M1$	$(1.0\pm0.3)\times10^{-2}$	
			12±3	1		if $E2$	3.3±1.3	
						if $M1$	$(8\pm3)\times10^{-3}$	
			14±3	3		$(M1)$	0.17±0.06	
			4±1	5		$(M1)$	0.10±0.04	
11	4^+	3620	18±4	1		$E2$	$1.4_{-0.7}^{+1.1}$	19_{-9}^{+15}
			82±4	2	0.14±0.17	$E2$	3_{-3}^{+7}	40_{-40}^{+100}
						$M1$	$0.10_{-0.05}^{+0.08}$	
13	2^+	3898	22±2	0		$E2$	0.44±0.07	6.0±1.0
			68±2	1	0.0±0.1			
						$M1$	$(4.4\pm0.6)\times10^{-2}$	
			5±2	3		$(M1)$	$(3.4\pm1.5)\times10^{-2}$	
			5±2	4		$(M1)$	$(5\pm2)\times10^{-2}$	
14	2^+	4107	43±6[b]	0		$E2$	0.24±0.05	3.3±7.0
			57±6[b]	1	0.09±0.12	$M1$	$(1.0\pm0.2)\times10^{-2}$	
					or			
					$-2.8_{-1.7}^{+0.8}$	$E2$	2.4±0.6	
						$M1$	$(1.1_{-0.6}^{+1.3})\times10^{-3}$	
					or			
			51±2[c]	0		$E2$	0.28±0.04	3.8±0.5

TABLE III (*Continued*)

Level	J^π	Level energy (keV)	Decay mode % decay	To level	Multipole mixing ratio	σL	$\lvert M\rvert^2$[Weisskopf units (W.u.)]	$B(E2)$ (e^2 fm^4)
			32±2[c]	1	$0.73_{-0.11}^{+0.17}$	$E2$	0.54±0.17	7.3±2.3
						$M1$	$(3.7\pm0.9)\times10^{-3}$	
			5±3[c]	2		$E2$	2.6±1.6	35±22
			5±2[c]	3		if $E2$	7.6±3.0	
						if $M1$	$(7\pm3)\times10^{-3}$	
			5±2[c]	4		if $E2$	12.5±5	
						if $M1$	$(10\pm4)\times10^{-3}$	
			2±1[c]	8		($M1$)	$(2\pm1)\times10^{-2}$	
21	3^-	4475		1 (mainly)		$E1$	$(1.1_{-0.3}^{+0.8})\times10^{-3}$	
^{60}Ni								
2	2^+	2160	16±3	0		$E2$	<0.1	<1.5
			84±6	1	−1.2±0.3	$E2$	<33	<470
						$M1$	$<9\times10^{-3}$	
^{62}Ni								
3	2^+	2300	62±3[c]	0		$E2$	0.5±0.15	7.1±2.2
			38±3[c]	1	$-(1.7_{-0.5}^{+0.9})$	$E2$	7.7±2.7	114±40
					or	$M1$	$(1.9_{-1.0}^{+1.6})\times10^{-3}$	
					−0.07±0.18	$E2$	≤0.3	≤4.5
						$M1$	$(7.2_{-1.9}^{+2.4})\times10^{-3}$	

[a] Reference 32.
[b] References 8 and 9.
[c] Reference 7.

errors quoted on the lifetimes include both the errors in the measured $F(\tau)$ and those due to uncertainties in the calculation of the $F(\tau)$ curve.

B. Matrix Elements and Transition Strengths

The mean life τ of an excited state is related to its total width Γ by the relation

$$\Gamma=\hbar/\tau=\sum_i \Gamma_i, \qquad (4.1)$$

where Γ_i are the partial widths for the various decay modes. The partial widths for internal conversion of high-energy $E2$ and $M1$ γ rays are negligible.[34] The conversion coefficients are less than 10^{-3} and were neglected in the extraction of the matrix elements. Electric monopole decay of states of spin J to other states of the same spin has been discussed by Church and Weneser.[35] Their calculations, and their review of the rather limited experimental data, indicate that in the nickel isotopes the partial width for $E0$ decay is at least one order of magnitude, and probably two or more orders of magnitude, smaller than the partial width for $E2$ radiative decay.

The electromagnetic decay properties of ^{58}Ni have been studied extensively by Van Patter, Horoshko, and Hinrichsen,[8] and others at the Bartol Research Foundation,[9–10] and by Start *et al.*[7] at Oxford University. These two groups have determined spins and measured branching ratios and $E2/M1$ mixing ratios using $(p, p'\gamma)$ angular correlation techniques. The Bartol group also obtained spin and mixing ratio assignments from γ-ray angular distributions and statistical reaction theory. Spins and parities have also been assigned by Jarvis *et al.*[12] on the basis of inelastic α-particle scattering data. References to earlier work can be found in Refs. 9–12.

The spin assignments made by the three groups are in agreement with the exception of the 3.531-MeV

[34] L. A. Sliv and I. M. Band, in *Coefficients of Internal Conversion of Radiation* (Physics Technical Institute, Academy of Sciences, Leningrad, 1956), Part I, K shell [issued in USA as University of Illinois Report No. 57 ICC-KI (unpublished)]; M. E. Rose, *Internal Conversion Coefficients* (North-Holland Publishing Co., Amsterdam, 1958).

[35] E. L. Church and J. Weneser, Phys. Rev. **103**, 1035 (1965).

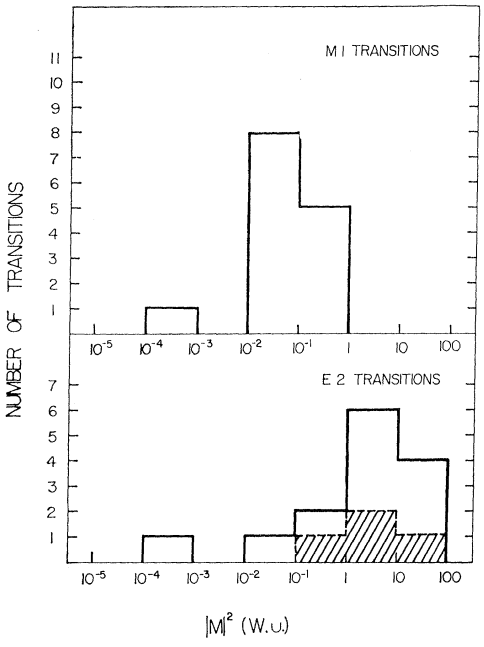

FIG. 10. Systematics of electromagnetic transition strengths in ^{58}Ni. The shaded region indicates transition strengths determined from Coulomb excitation (Refs. 13 and 14) and inelastic scattering (Refs. 12, 37, and 38) experiments.

state which is assigned $J^\pi=(0^+)$ by Van Patter *et al.*[8], and $J^\pi=4^+$ by Jarvis *et al.*[12] The branching and mixing ratios are also generally in good agreement, although there appears to be a small systematic error in the branching ratios.[7,8] The two branching ratio measurements disagree most for high-energy transitions from high-lying states. Although the differences are occasionally outside of experimental error, the discrepancy is large only in the case of the 4.107-MeV level. Table III summarizes the decay properties of levels in ^{58}Ni and of the second 2^+ states in ^{60}Ni and ^{62}Ni. All the ^{58}Ni level energies and lifetimes are from the present work, except as otherwise indicated in the Table. The spin assignments quoted for the ^{58}Ni levels are from Refs. 7–9. Parity assignments are from Refs. 7–12. In view of the possible systematic error in the branching ratios mentioned above, the values of the branching ratios adopted in Table III are simple averages of the data of Refs. 7–9. The errors have been made large enough to include all the measured values. The mixing ratios in Table III are averages of the available data weighted inversely as the square of the error.

The ^{60}Ni γ-decay data come from the γ-γ angular correlation work of Shafroth and Wood.[36] The decay modes of the ^{62}Ni 2^+_2 state were studied by Start *et al.*[7] The value of the mixing ratio for the $2^+_2\rightarrow 2^+_1$ decay is ambiguous in this work; the values $\delta=-0.07_{-0.15}{}^{+0.18}$ (mostly $M1$ radiation) and $\delta=-1.7_{-0.5}{}^{+0.9}$ (mostly $E2$ radiation) give equally good fits to the data. The latter value is more consistent with the magnitude of the mixing ratios of $2^+_2\rightarrow 2^+_1$ transitions in ^{58}Ni and ^{60}Ni.

V. DISCUSSION

A. Systematics

The matrix elements which have been extracted from the ^{58}Ni lifetime data are shown in the histogram of Fig. 10. The shaded regions represent the transition rates measured by Coulomb excitation[13,14] and inelastic scattering.[37,38] Transition rates have also been calculated from the deformation parameters obtained in a distorted-wave Born-approximation (DWBA) analysis of inelastic α particle scattering.[12] These results, as well as those obtained from the analysis of inelastic electron and α-particle scattering, are compared with the present work in Table IV. The only disagreement occurs in the case of $B(E2)$ values extracted from inelastic α-particle scattering cross sections. While the lifetime measurements yield what is unquestionably an electromagnetic transition probability, the inelastic scattering work may be more sensitive to nuclear effects.

The values of $|M|^2$ shown in Table III are consistent with positive-parity assignments for all the levels of ^{58}Ni for which partial widths were extracted (excepting the 3^- state at 4.475 MeV). Quadrupole transitions between states of opposite parity are $M2$, rather than $E2$, transitions. The values of $|M|^2$ for $E2$ transitions for the observed quadrupole transitions range from 2.6×10^{-2} to 15. If these were $M2$ transitions, the values of $|M|^2$ would be a factor of 50 larger. No $M2$ transitions with enhancement greater than 10 single-particle units have previously been reported in compilations of transition rate systematics by Wilkinson,[39] Skorka *et al.*,[40] and Gove.[41] The systematics of $E1$ transition strengths have been tabulated by Perdrisat.[42] No $3^-\rightarrow 2^+$ transition rates of the type reported here have been measured, but other types of $E1$ transitions are usually strongly retarded.

B. Comparison with Theory

In the absence of sufficient data concerning transition rates, theoretical considerations of the nuclear structure of the nickel isotopes have largely been concerned with fitting excitation energy, spin, and parity data for low-lying states. Shell-model and vibrational-model approaches have been reasonably successful and

[36] S. M. Shafroth and G. T. Wood, Phys. Rev. **149**, 827 (1966).

[37] M. A. Duguay, C. K. Bockelman, T. H. Curtis, and R. A. Eisenstein, Phys. Rev. **163**, 1259 (1967).

[38] H. Crannell, R. Helm, H. Kendall, J. Oesser, and M. Yearian, Phys. Rev. **123**, 923 (1961).

[39] D. H. Wilkinson, in *Nuclear Spectroscopy*, edited by F. Ajzenberg-Selove (Academic Press Inc., New York, 1960).

[40] S. J. Skorka, J. Hertel, and T. W. Retz-Schmidt, Nucl. Data **2**, 347 (1966).

[41] N. B. Gove, in *Nuclear Spin-Parity Assignments*, edited by N. B. Gove (Academic Press Inc., New York, 1966).

[42] C. Perdrisat, Rev. Mod. Phys. **38**, 41 (1966).

TABLE IV. Comparison of transition strengths in ^{58}Ni as measured by inelastic α-particle and electron scattering and by Doppler-shift-attenuation methods.

Transition	$\lvert M \rvert^2$ (W.u.) (α, α')[a]	(e, e')[b]	(e, e')[c]	Doppler shift
$1454(2^+) \rightarrow 0(0^+)$	14.4 ± 0.15	14.3 ± 1.9	9.8	10 ± 1.3
$3037(2^+) \rightarrow 0(0^+)$	1.0 ± 0.2		1.2	1.7 ± 0.3
$3263(2^+) \rightarrow 0(0^+)$	1.4 ± 0.3	4.5 ± 1.6	2.3	2.8 ± 0.5
$3898(2^+) \rightarrow 0(0^+)$	$0.4 \rightarrow 0.1$			0.44 ± 0.07

[a] Reference 12.
[b] Reference 38.
[c] Reference 37. The error in $\lvert M \rvert^2$ is estimated to be $\pm 15\%$ and is largely due to uncertainties in the description of transition charge densities.

both approaches were able to account for the previously measured transition rates for the decay of the 2^+_1 states. The application of the vibrational model to the nickel isotopes would seem to be a legacy of history, based on a resemblance of energy spectra to the classic "one-phonon" 2^+_1, "two-phonon" 0^+_2, 2^+_2, 4^+_1 triplet ordering of the levels. This model encounters difficulty in explaining the decay properties of the "two-phonon" 2^+_2 states, which decay to the 2^+_1 state with appreciable $M1$ strength. Furthermore, the model in a simple form cannot be expected to deal adequately with the positions and decay properties of higher states. Shell-model approaches, especially those which include core effects, show promise in their ability to fit energy spectra and transition probabilities, although the promise is far from being fulfilled.

Recent shell-model calculations for the nickel isotopes[1-4] have generally assumed a closed ^{56}Ni core and valence neutrons in the $p_{3/2}$, $f_{5/2}$, and $p_{1/2}$ shells. A variety of potentials have been used in attempts to describe the residual interaction. Many of these have been phenomenological[1-4]; some calculations[1,2] have used χ^2 fitting of energy level spectra to determine the two-body matrix elements. It may be noted that several calculations with "realistic" nucleon-nucleon potentials did not give acceptable fits to the level spectra.[1,3] However, a recent calculation by Gambhir,[43] using a Hamada-Johnston potential, has given somewhat better fits than the earlier work. The existence of finite electric transition rates is explained by core polarization and the resulting "effective charge" of the valence neutrons. In most calculations, this effective charge has been assumed constant for all transitions. The agreement between theory and experiment is generally poor, as can be seen from the comparison of $B(E2)$ values for the decay of the 2^+_1 and 2^+_2 states of ^{58,60,62}Ni, shown in Table V. All calculated $B(E2)$ values have been normalized to unit effective charge.

Auerbach[2] and Cohen *et al.*[1] calculated the ratio $B(E2\colon 2^+_2 \rightarrow 0^+_1)/B(E2\colon 2^+_2 \rightarrow 2^+_1)$ using matrix elements obtained from a fit to energy level spectra. In ^{58}Ni, they both find the ratio to be about 30 compared with the experimental result of $(1.8 \pm 0.3) \times 10^{-3}$. This rather striking discrepancy has led Federman and Zamick[44] to examine the sensitivity of the $B(E2)$ values to the two-body residual interactions used. The ^{58}Ni calculation was redone using matrix elements computed by Lawson, MacFarlane, and Kuo[45]; the resulting $B(E2)$ ratio was 0.51. Furthermore, it was found that changing Auerbach's $\langle (p_{3/2}p_{1/2})^{J=2} \mid V \mid (p_{3/2}{}^2)^{J=2} \rangle$ matrix element from 0.83 to 0.5 MeV increased the ratio to 0.69, while not significantly affecting the calculated level spectrum. The individual transition strengths are also in better agreement with experiment. Although good agreement with experiment has still not been obtained, this work indicates that the $B(E2)$ values are, in fact, quite sensitive to the choice of two-body matrix elements.

Federman and Zamick[44] have also examined the state dependence of the effective charge to determine the extent to which the assumption of a single effective charge for all transitions in ^{58}Ni is an oversimplification. They find that while the neutron effective charge for a ^{56}Ni core may vary from 0.73 ($p_{3/2} \rightarrow p_{3/2}$ or $p_{1/2} \rightarrow p_{3/2}$ transition) to 1.14 ($f_{5/2} \rightarrow f_{7/2}$ transition), the calculated transition rates still cannot be brought closer to the experimental values. One transition that can be understood in a shell-model framework with core excitation is the highly retarded $E1$ decay $3^-_1 \rightarrow 2^+_1$. The simplest shell-model configurations for these states are $(g_{9/2}p_{3/2})^{J=3-}$ and $(p_{3/2}{}^2)^{J=2+}$. However, in a single-particle transition between these configurations both the orbital and total angular momentum of the transition nucleon change by at least 3. Therefore the $E1$ decay must go by admixtures of particle-hole configurations in the wave functions of the 3^- and 2^+ states. For example, a component of $(p_{3/2}{}^2 g_{9/2} f_{7/2}{}^{-1})^{J=3-}$ in the wave function of the 3^- state would explain this transition.

The poor agreement between theory and experiment in ^{58}Ni results partly from the improper treatment of core excited states. As more neutrons are added out-

[43] Y. K. Gambhir, Phys. Letters **26B**, 695 (1968).
[44] P. Federman and L. Zamick, Phys. Rev. (to be published).
[45] R. D. Lawson, M. H. MacFarlane, and T. Kuo, Phys. Letters **22**, 168 (1968).

TABLE V. Comparison of calculated and experimental $B(E2)$'s for the 2_1^+ and 2_2^+ states of ^{58}Ni, ^{60}Ni, and ^{62}Ni.

Transition	Experiment	$B(E2)$ (e^2 fm^4) Ram Raj *et al.*[a]	Arvieu and Salusti[b]	Auerbach[c]	Federman and Zamick[d]
^{58}Ni $2_1^+\rightarrow 0_1^+$	136±18		62	97	
$2_2^+\rightarrow 0_1^+$	0.36±0.14		3	17.5*	9.5
$2_2^+\rightarrow 2_1^+$	200±70		20	0.61*	16.0
$2_2^+\rightarrow 0_1^+$ / $2_2^+\rightarrow 2_1^+$	$(1.8\pm0.3)\times10^{-3}$		0.15	29*	0.59
^{60}Ni $2_1^+\rightarrow 0_1^+$	194±16[e]	57	118	165	
$2_2^+\rightarrow 0_1^+$	<1.5	0.62	1.8	5	
$2_2^+\rightarrow 2_1^+$	<470	25	0.6	225	
^{62}Ni $2_1^+\rightarrow 0_1^+$	168±16[e]	67	174	204	
$2_2^+\rightarrow 0_1^+$	7.1±2.2	0.44	1.8	0.24	
$2_2^+\rightarrow 2_1^+$	114±40[f]	23	0.08	309	

[a] Reference 4.
[b] Reference 6.
[c] Reference 2. The ^{58}Ni reduced matrix elements marked by an asterisk are those recalculated by Federman and Zamick (Ref. 44) from the same matrix elements and effective charge used by Auerbach (Ref. 2).
[d] Reference 44.
[e] References 13 and 14.
[f] Assuming the larger value of $2_2^+\rightarrow 2_1^+$ mixing ratio from Ref. 7.

side the ^{56}Ni core, the effect of core excitations on the transition rates should diminish. To some extent this result is reflected in the work of Auerbach[2] and Cohen *et al.*[1] While agreement with experiment is still limited to order of magnitude results, the trends are more correctly predicted in ^{60,62}Ni than in ^{58}Ni.

Substantial evidence for core excitations exists. Cosman *et al.*[33] [^{58}Ni$(d, p)^{59}$Ni], Bassani *et al.*[46] [^{58}Ni$(p, t)^{56}$Ni], and Fulmer and Daehnick[47] [^{60}Ni$(d, t)^{59}$Ni] have all found evidence consistent with the existence of $1f_{7/2}$ holes in the ground states of the even nickel isotopes. Hiebert *et al.*[48] used the ^{63}Cu$(d, {}^3\mathrm{He})^{62}$Ni reaction to study proton particle-hole states in ^{62}Ni; they found that the wave functions of the one- and two-phonon states contained roughly 25% admixtures of $(1f^{-1}_{7/2}, 2p_{3/2})$ configurations. Glover and Douglas[49] studied the closure of the neutron shell at $N=28$ by the ^{46,48}Ca$(t, p)^{48,50}$Ca reactions. Their results are consistent with (20–30)% admixture of $2p_{3/2}{}^2$, $1f_{5/2}{}^2$, and $2p_{1/2}{}^2$ configurations in the ground state of ^{48}Ca. The difficulty that exists in the theoretical description of transition rates in the nickel isotopes is one common to all shell-model calculations, namely, the correct choice of residual interaction and basis states. The nucleus ^{18}O is similar to ^{58}Ni in that it has two neutrons outside a doubly closed shell. Engeland[50] and Benson and Irvine[51] have calculated transition rates in ^{18}O; they were able to obtain agreement with experiment only after core excitations were properly handled.

VI. CONCLUSIONS

Although the Doppler-shift-attenuation method has been applied by many workers to the measurement of lifetimes in many nuclei, only recently has the question of nuclear stopping become important. The present check on the stopping power theory of LSS for nickel ions in nickel and the large-angle scattering formulation of Blaugrund gives considerable confidence that $F(\tau)$ curves, and hence lifetimes, extracted from these formulations are correct.

The wave functions used in the theoretical transition probability calculations have been derived in the absence of detailed experimental γ-decay information and with the prime purpose of reproducing energy spectra. It is, therefore, not surprising that theoretical and experimental transition probabilities do not agree. In addition, it would seem that core excitations will play an important role in determining transition probabilities in ^{58}Ni, and these have not yet been properly taken into account.

Lifetimes extracted from inelastic scattering studies show general agreement with the present DSA results. It may be, however, that the existing differences will prove a sensitive test of the wave-function components.

[46] G. Bassani, N. M. Hintz, and G. D. Kavaloski, Phys. Rev. **136**, 1006 (1964).
[47] R. H. Fulmer and W. W. Daehnick, Phys. Rev. **139**, B579 (1965).
[48] J. C. Hiebert, E. Newman, and R. H. Bassel, Phys. Letters **15**, 160 (1965).
[49] R. N. Glover and A. C. Douglas, Phys. Letters **25B**, 333 (1966).
[50] T. Engeland, Nucl. Phys. **72**, 68 (1965).
[51] H. G. Benson and J. M. Irvine, Proc. Phys. Soc. (London) **89**, 249 (1966).

ACKNOWLEDGMENTS

We acknowledge the assistance of J. Audesirk, L. Guthman, S. Harrison, and J. Tape in accumulating the data. We are grateful to Dr. Start, Dr. Hinrichsen, and Dr. Van Patter for communicating their results prior to publication. We also thank Professor A. Arima, Professor L. Zamick, and Professor P. Federman for many enlightening discussions.

APPENDIX

The major uncertainty encountered in computing the attenuation factor is that associated with the stopping power expressions. To estimate the error introduced into the lifetime by this error, one may allow the electronic and nuclear stopping expressions to be multiplied by the constant factors f_e and f_n, respectively. The total specific energy loss then becomes

$$dE/dx=f_n[(dE/dx)_n+f(dE/dx)_e], \qquad \text{(A1)}$$

where $f=f_e/f_n$. For clarity, the expressions for the recoil time $t(E)$, large-angle scattering correction $\cos\phi_b(E)$,[21] and attenuation factor $F(\tau)$ are summarized:

$$t(E)=\int_{E_i}^{E}\frac{dE}{v(dE/dx)}=t(E,k),$$

$$\cos\phi_b=\exp\left(-\frac{G(r)}{2r}\int_{E_i}^{E}\frac{(dE/dx)_n}{dE/dx}\frac{dE}{E}\right)=\cos\phi_b(k),$$

$$F(\tau)=\frac{1}{v_i\tau}\int_{E_i}^{0}\frac{\cos\phi_b e^{-t/\tau}}{dE/dx}dE=F(\tau,k). \qquad \text{(A2)}$$

The electronic energy-loss expression used was that of LSS, $(d\epsilon/d\rho)_e=-k\epsilon^{1/2}$. Thus, multiplication by f_e and f_n leads to the transformed expressions

$$t(E,k)\rightarrow t(E,fk)/f_n,$$
$$\cos\phi_b(k)\rightarrow\cos\phi_b(fk),$$
$$F(\tau,k)\rightarrow F(f_n\tau,fk). \qquad \text{(A3)}$$

The relative importance of f_e and f_n in shifting the $F(\tau)$ curve depends on the relative amounts of electronic and nuclear energy loss. If most of the recoil energy is lost in electronic collisions, i.e., $\epsilon_i\gg1$ (large initial recoil energy), $F(\tau)$ is insensitive to the nuclear stopping contribution and hence to f_n. Conversely, if most of the energy is lost in nuclear collisions, i.e., $\epsilon_i\sim1$ (low initial recoil energy), $F(\tau)$ is insensitive to f_e. When roughly equal amounts of energy are lost in both types of collisions, the attenuation factor is sensitive to both f_e and f_n. The effect on the $F(\tau)$ curve in this case is greatest when f_e-1 and f_n-1 have opposite signs.

To understand this last effect, assume that f_e and f_n may take the values $1\pm\Delta$. Note that for $f_e=f_n$, i.e., $f=1$, the $\cos\phi_b$ term is unaffected by the changes in the stopping expressions. All changes in $F(\tau)$ are due to the differences in slowing down time. When $f_e=1\pm\Delta$ and $f_n=1\mp\Delta$, the change in the electronic stopping term is in the opposite direction from the change in the nuclear stopping term and the total energy loss is roughly unaffected; most of the changes in $F(\tau)$ are due to differences in $\cos\phi_b$. Thus, large angle scattering is the dominant factor in attenuating the z component of the velocity for low initial recoil velocities.

The three measurements of the lifetime of the first excited state of ^{58}Ni tested the stopping-power expressions under the different stopping conditions discussed above. Table I summarizes the fraction of energy lost in nuclear collisions and the measured lifetimes. The parameters f_e and f_n were varied until the measured attenuation factors no longer yielded lifetimes within the range spanned by the Coulomb excitation measurement. Changes of up to 15% in the stopping cross sections (f_e and f_n varying from 0.85 to 1.15) gave results consistent with the Coulomb excitation value. Errors in the other lifetimes due to uncertainties in the stopping cross sections were obtained from $F(\tau)$ curves calculated with $f_e=1\pm0.15$ and $f_n=1\mp0.15$.